DOI: 10.1002/anie.201411944

A Functionalized Ag_2S Molecular Architecture: Facile Assembly of the Atomically Precise Ferrocene-Decorated Nanocluster $[Ag_{74}S_{19}(dppp)_6(fc(C\{O\}OCH_2CH_2S)_2)_{18}]$**

*Yiyi Liu, Bahareh Khalili Najafabadi, Mahmood Azizpoor Fard, and John F. Corrigan**

Abstract: *A ferrocene-based dithiol 1,1′-$[fc(C\{O\}OCH_2CH_2SH)_2]$ has been prepared and treated with a Ag^I salt to form the stable dithiolate compound $[fc(C\{O\}OCH_2CH_2SAg)_2]_n$ ($fc = [Fe(\eta^5\text{-}C_5H_4)_2]$). This is used as a reagent for the preparation of the nanocluster $[Ag_{74}S_{19}(dppp)_6(fc(C\{O\}OCH_2CH_2S)_2)_{18}]$ which was obtained in good yield (dppp = 1,3-bis(diphenylphosphino)propane).*

The chemistry, materials, and biomaterials science of atomically precise Ag_2S nanoclusters is currently at the forefront of research. Interest in these frameworks has continued to develop since the early preparation of Ag_2S clusters and the investigation of their photophysical properties when bound as guest molecules in zeolitic hosts, a progression which has mirrored the development of larger, nanoscopic frameworks.[1] Ag_2S nanoparticles and nanoclusters continue to attract interest as a result of their optical properties, their structural diversity, and their potential applications. The exciton Bohr radius of Ag_2S is approximately 2.2 nm and nanoscale assemblies of this material display photoluminescence in the near-infrared region of the electromagnetic spectrum.[2] This has led to several reports of Ag_2S quantum dots as novel near-infrared photoluminescent materials for bioimaging in living systems.[3] This environmentally benign material has also attracted interest for photovoltaic applications[4] and because of the fact that silver(I)-based metal–sulfide heterostructures can also display interesting dual photoemission from the two components in the materials.[4b,5] From a structural perspective, Fenske and co-workers have developed an extensive library of crystallographically characterized Ag_2S frameworks, including the molecular structure of the largest silver sulfide cluster reported to date, $[Ag_{490}S_{188}(SC_5H_{11})_{114}]$.[6]

At a more fundamental level, the structurally characterized nanocluster $[Ag_{62}S_{13}(S^tBu)_{32}]^{4+}$ [7] was reported as the first example of such a large, molecular system displaying luminescence both in solution and in the solid state. The photophysics of the cluster were recently cemented by Zhu and co-workers[8] with an in-depth structure–property relationship study of it and the related framework $[Ag_{62}S_{12}(S^tBu)_{32}]^{2+}$, which contains a "metallic" core. These studies complement recent findings showing how silver–thiolate surfaces can stabilize larger Ag cores in atomically precise nanoclusters.[9]

In addition to their optical properties, the stabilization of the surfaces in these clusters with thiolate ligands offers an opportunity to incorporate specific chemical properties into the frameworks.[10] With this in mind, the incorporation of multiple ferrocenyl units onto nanoclusters of Ag_2S was reported in 2010.[11] The targeted synthesis of polyferrocenyl assemblies on inorganic supports is attracting significant research focus because of the electrochemical properties of the frameworks, which offer potential applications as redox-active and/or luminescent sensors,[12] and as electrode materials.[13] In metal cluster chemistry, supports for such assemblies include the aforementioned metal–chalcogen frameworks,[11,14] gold nanoparticles,[12a,15] polyoxometalates[16] and, recently, tin–chalcogenide clusters as developed by Dehnen and co-workers.[17]

We had previously prepared the reagent $Fc(C\{O\}OCH_2CH_2SSiMe_3)$ ($Fc = [CpFe(C_5H_4)]$), which, when treated with silver acetate and $S(SiMe_3)_2$, yielded surface functionalized, high-nuclearity Ag_2S clusters with ferrocene-rich surfaces.[18] Despite their apparent size monodispersity single crystals proved elusive, however through the combination of high-resolution TEM (HRTEM) and additional analytical methods, idealized molecular formulae including $[Ag_{36}S_9(SCH_2CH_2O\{O\}CFc)_{18}(PPh_3)_3]$ could be derived.[18] These formulations are in keeping with data obtained for the crystallographically characterized $[Ag_{48}S_6(SCH_2Fc)_{36}]$ which contains a shorter tether between the ferrocenyl units and the surface thiolate ligands.[11] However, the retention of more functionalized ferrocenyl units is important in the context of developing sensitivity towards analytes[12,19] and using Ag_2S as a monodisperse support in this regard has tremendous potential. We speculated that the preparation of bidentate ferrocenyl–chalcogen

---

[*] Y. Liu, B. Khalili Najafabadi, M. Azizpoor Fard,
Prof. Dr. J. F. Corrigan
Department of Chemistry, The University of Western Ontario
London, Ontario, N6A 5B7 (Canada)
E-mail: corrigan@uwo.ca
Prof. Dr. J. F. Corrigan
Centre for Advanced Materials and Biomaterials Research
The University of Western Ontario
London, Ontario, N6A 5B7 (Canada)

[**] We thank the Natural Sciences and Engineering Research Council (NSERC Canada) for financial support for this research. The Canada Foundation for Innovation, NSERC, and the University of Western Ontario are also acknowledged for equipment funding. The authors thank Dr. M. Hessari for the help with cyclic voltammetry experiments. Some research described in this paper was performed using beamline 08B1-1 at the Canadian Light Source, which is supported by the Canada Foundation for Innovation, NSERC, the National Research Council Canada, the Canadian Institutes of Health Research, the Government of Saskatchewan, Western Economic Diversification Canada, and the University of Saskatchewan.
dppp = 1,3-bis(diphenylphosphino)propane; $fc = [Fe(\eta^5\text{-}C_5H_4)_2]$.

Supporting information for this article is available on the WWW under http://dx.doi.org/10.1002/anie.201411944.

reagents would limit surface flexibility and lead to an increased stability/rigidity of the corresponding clusters, thus permitting the formation of single crystals suitable for X-ray diffraction analysis. Herein, we describe a surprisingly facile route to the nanoscale cluster $[Ag_{74}S_{19}(dppp)_6(fc(C\{O\}OCH_2CH_2S)_2)_{18}]$ (**1**) (dppp = 1,3-bis(diphenylphosphino)propane; fc = $Fe(\eta^5\text{-}C_5H_4)_2$) which was obtained in good yield. The structural characterization of **1** by single-crystal X-ray diffraction is also reported.

One useful strategy to access to Ag/S/SR clusters involves the addition of "S^{2-}" to a preformed silver(I) thiolate coordination polymer $[AgSR]_n$. Convenient sources of the sulfide ion include the use of CS_2 and $S(SiMe_3)_2$.[6,20] The development of tailored $[AgSR]_n$ polymers offers an avenue through which a specific functional group might be readily incorporated onto a Ag_2S cluster. In this vein, $[fc(C\{O\}OCH_2CH_2SAg)_2]_n$ (**2**) was prepared from 1,1′-$[fc(C\{O\}OCH_2CH_2SH)_2]$ upon reaction with two equivalents of $AgSO_3CF_3$, which was then used as a precursor for cluster **1**. The dithiol 1,1′-$[fc(C\{O\}OCH_2CH_2SH)_2]$ itself can be conveniently prepared from 1,1′-$[fc(C\{O\}Cl)_2]$ (Scheme 1 and Supporting Information).

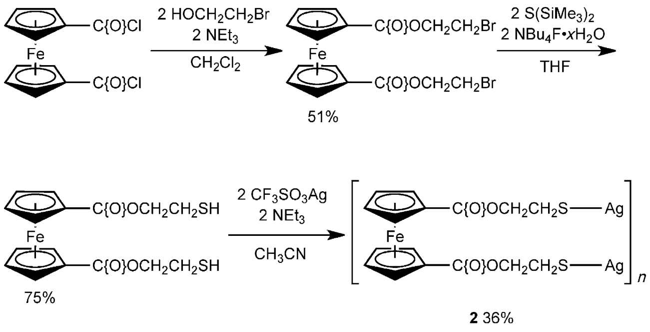

Scheme 1. Synthesis of $[fc(C\{O\}OCH_2CH_2SAg)_2]_n$ **2**.

Although insoluble in all common organic solvents, $[fc(C\{O\}OCH_2CH_2SAg)_2]_n$ (**2**) can be dissolved with excess dppp (2 equiv) in CH_2Cl_2. Treatment of these solutions with $S(SiMe_3)_2$ (0.3 equiv) at room temperature proceeds with a color change from orange to dark red. Layering reaction solutions with diethyl ether lead to the selective isolation of the cluster $[Ag_{74}S_{19}(dppp)_6(fc(C\{O\}OCH_2CH_2S)_2)_{18}]$ (**1**) in high yield as dark red crystals with other side products left in solution.

Cluster **1** was analyzed by single-crystal X-ray diffraction to elucidate its structural features (Figure 1). Single crystals of **1** are highly solvated and only weakly diffracting. Although a structural model of the Ag_2S core could be obtained from diffraction data using a conventional, sealed-tube X-ray source, data suitable to refine the entire structure and thus the surface characteristics required a brighter source and were collected using a synchrotron beam line at the Canadian Light Source (18 keV; $\lambda = 0.68877$ Å). Cluster **1** was solved and refined in the space group $R\bar{3}$; a central sulfide resides about a crystallographic $\bar{3}$ site. All Ag, S, P, and (non-disordered) Fe atoms were refined anisotropically whereas all

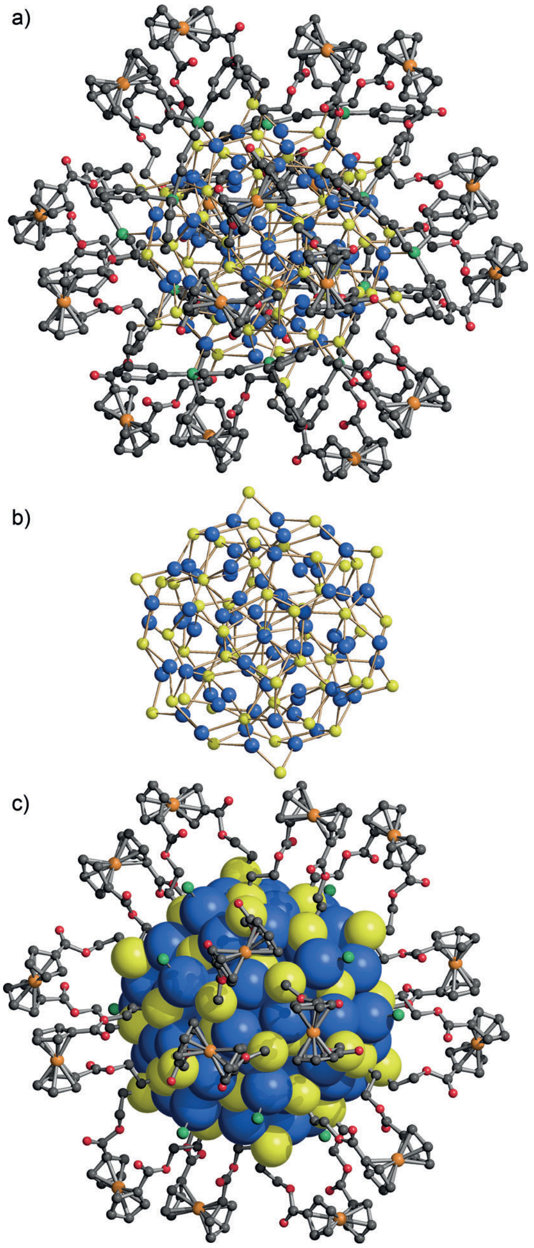

Figure 1. a) Ball-and-stick diagram of the molecular structure of $[Ag_{74}S_{19}(dppp)_6(fc(C\{O\}OCH_2CH_2S)_2)_{18}]$ (**1**). H atoms have been omitted for clarity. b) Ball-and-stick diagram of the $Ag_{74}S_{55}$ core of **1**. c) Space-filling diagram of the $Ag_{74}S_{55}$ core with the C atoms of dppp omitted to show the distribution of ferrocenyl ligands in **1**. Atom colors in (a–c): Ag = blue, S = yellow, P = green, O = red, Fe = orange, C = gray.

C and O atoms were refined isotropically. One of the three crystallographically independent ferrocenyl units (thus six of the eighteen) displayed disorder. A two-site model for the ferrocenyl dithiolate ligand "Fe1" was satisfactorily refined with 50:50 occupancy. For clarity, the disorder is not shown in Figure 1.

The rather symmetrical $Ag_{74}S_{55}$ core ($\approx 1.7 \times 1.5 \times 1.4$ nm^3) of cluster **1** consists of seventy-four silver centers bonded to nineteen sulfide (S^{2-}) and thirty-six thiolate ligands (each 1,1′-$[fc(C\{O\}OCH_2CH_2S)_2]^{2-}$ providing two). The overall dimensions of **1** (including the ferrocenyl shell) are approximately 3.1 × 3.0 × 3.0 nm^3. The central sulfide adopts a μ_8-bridging coordination model whereas the other 18 sulfides form μ_6 bridges to Ag centers. Thirteen of the S^{2-} centers are arranged in a (non-bonded) centered icosahedral arrangement in the cluster core whereas the six additional S^{2-} centers are closer to the cluster surface. The surface thiolates form μ_2, μ_3, or μ_4 bridges to Ag atoms. The Ag^I centers in cluster **1** adopt three coordination geometries: distorted linear, trigonal planar, or distorted tetrahedral. The arrangement of the six dppp ligands at the cluster surface can be described as being at the corners of an octahedron if each $\widehat{PP}$ is considered as occupying one vertex position.

Of the eighteen $[fc(C\{O\}OCH_2CH_2S)_2]^{2-}$ ligands, the twelve that were not disordered display a conformation with the two substituents of the two cyclopentadienyl rings rotated at angle of circa 31.5° with respect to each other along the C_5–Fe–C_5 axis (Figure 1). The two C=O moieties of the $[fc(C\{O\}OCH_2CH_2S)_2]^{2-}$ are oriented in the same direction and are essentially coplanar with their respective C_5 rings to which they are bonded. The two C_5 rings themselves are close to being parallel. The six disordered $[fc(C\{O\}OCH_2CH_2S)_2]^{2-}$ were satisfactorily refined with the C=O oriented in opposite directions on the two C_5 rings.

Silver–sulfide bond lengths for **1** range between 2.381(7)–2.968(7) Å whereas those for silver–thiolate interactions measure between 2.372(7)–2.800(7) Å. Ag⋯Ag distances in the cluster fall within the range 2.901(3)–3.374(3) Å. Similar distances/bond lengths are reported for the comparably sized cluster $[Ag_{70}S_{16}(SPh)_{34}(PhCO_2)_4(triphos)_4]$ (triphos = 1,1,1-tris{(diphenylphosphino)methyl}ethane).[21] Ag⋯Ag distances for **1** confirmed that there is no significant Ag–Ag interaction,[22] consistent with the +1 oxidation state assigned for all silver centers. The space-filling model (see the Supporting Information) clearly demonstrates how the ligands effectively shield the $Ag_{74}S_{55}$ core and also shows clearly how the 1,1′-$[fc(C\{O\}O)_2]$ units remain exposed at the cluster surface.

Although crystals of **1** are poorly soluble in organic solvents, they do dissolve in CH_2Cl_2 in sufficient concentrations for analysis by cyclic voltammetry (≈ 0.003 mM). One quasi-reversible redox wave ($i_{pa}/i_{pc} \approx 1.1$; where i_{pa} is the anodic peak current and i_{pc} is the cathodic peak current) is detected with the $E_{1/2}$ value ($E_{1/2} = (E_{pa} + E_{pc})/2$) at 949 mV and a ΔE value ($\Delta E = |E_{pa} - E_{pc}|$) of 168 mV (vs. Ag/AgCl; scan rate = 100 mV s^{-1}). The redox wave can be assigned to the one-electron oxidation/reduction of the iron centers of the ferrocenyl moieties and the peak potentials are similar to those detected for $[fc(C\{O\}OCH_2CH_2Br)_2]$ ($E_{1/2} = 980$ mV; see the Supporting Information).[12a,15] The shape and reversibility of the redox wave for the solution of **1** suggest that the molecular architecture remains intact upon oxidation of these Fe^{II} centers and that there is limited absorption of the cluster onto the electrode surface, unlike what was detected for $[Ag_{36}S_9(SCH_2CH_2O\{O\}CFc)_{18}(PPh_3)_3]$.[18]

The formation and characterization of **1** demonstrates a straightforward approach for the surface modification of Ag_2S nanoclusters and shows that bidentate ferrocenyl chalcogen reagents facilitate the structural characterization of such decorated nanoclusters by single-crystal X-ray diffraction. The preparation and isolation of **1** complements the employed synthetic strategy which uses silver thiolate polymers (AgSR) and $S(SiMe_3)_2$ as precursors for the preparation of high-nuclearity Ag_2S clusters.[6,20b] Use of this synthetic method offers potential to tune the R substituent in the nanocluster molecular design. We are further developing the reaction chemistry of $[fc(C\{O\}OCH_2CH_2SAg)_2]_n$ **2** and are investigating the preparation of other functionalized silver thiolates $[AgSR]_n$ for nanocluster formation.

Experimental Section

Synthesis of $[fc(C\{O\}OCH_2CH_2SH)_2]$: $[fc(C\{O\}OCH_2CH_2Br)_2]$ (0.41 g, 0.84 mmol) was dissolved in tetrahydrofuran (THF; 25 mL) and the solution was cooled to −10 °C. $S(SiMe_3)_2$ (0.53 mL, 2.5 mmol) was added, followed by tetrabutylammonium fluoride (TBAF; 0.48 g, 1.8 mmol) in THF (15 mL). The reaction was stirred for 10 min at −10 °C and the mixture was subsequently stirred at RT for 3.5 h. The solvent was removed under vacuum, and THF (35 mL) was used to dissolve the residue. Heptane (35 mL) was added to the flask and the majority of THF was then removed under vacuum. The orange solution was filtered through dry Celite to remove the precipitated salts and heptane was removed under vacuum to yield $[fc(C\{O\}OCH_2CH_2SH)_2]$ as a dark orange solid. Separation by flash chromatography on a silica gel column using ethyl acetate (EtOAc) as eluent can be used to purify the product; however, it was of sufficient purity to use for the preparation of **2** (below). Yield = 0.25 g (75 %). ^{1}H NMR (400 MHz, $CDCl_3$, 23 °C): $\delta = 4.85$ (m, 4H, CH), 4.45 (m, 4H, CH), 4.35 (t, $^3J = 6.4$ Hz, 4H, CH_2), 2.86 (dt, $^3J = 6.4$ Hz, $^2J = 8.0$ Hz, 4H, CH_2), 1.60 ppm (t, $^3J = 8.0$ Hz, 2H, SH); $^{13}C\{^1H\}$ NMR (100.5 MHz, $CDCl_3$): $\delta = 169.8$ (C(O)), 73.0 (CH), 72.4 (C), 71.7 (CH), 65.7 (CH_2), 23.5 ppm (CH_2); HRMS: m/z: calcd for $C_{16}H_{18}Fe_1O_4S_2$: 393.99961; found: 393.99860.

Synthesis of $[fc(C\{O\}OCH_2CH_2SAg)_2]_n$ **2**: To a solution of $fc(C\{O\}OCH_2CH_2SH)_2$ (0.23 g, 0.59 mmol) in CH_3CN (20 mL) was added a solution of $AgSO_3CF_3$ (0.38 g in 10 mL CH_3CN, 1.5 mmol). The mixture stirred rapidly for 5 min. NEt_3 (0.19 mL, 1.4 mmol) was added to the reaction mixture which resulted in the formation of an orange precipitate of $[fc(C\{O\}OCH_2CH_2SAg)_2]_n$. The orange precipitate was collected by filtration and washed with CH_3CN (4 × 10 mL). The solid was dried under vacuum. Yield = 0.13 g (36 %). Elemental analysis calcd. (%) for $C_{16}H_{16}O_4S_2Ag_2Fe$: C 31.62, H 2.65, S 10.52; found: C 32.25, H 2.76, S 9.67; m.p.: 173–177 °C.

Synthesis and characterization of $[Ag_{74}S_{19}(dppp)_6(fc(C\{O\}OCH_2CH_2S)_2)_{18}]$ **1**: The silver thiolate **2** (0.10 g, 0.16 mmol) was dissolved in CH_2Cl_2 (20 mL) with dppp (0.14 g, 0.33 mmol) by stirring for 1.5 h to yield an orange solution. $S(SiMe_3)_2$ (0.01 mL, 0.05 mmol) was then added and the reaction mixture was stirred for two hours at room temperature. The resultant solution was dark red in color. The mixture was layered with Et_2O (20 mL) and stored in subdued light for 3–4 days to yield dark-red single crystals of **1**. The structure was identified by X-ray crystallography to be $[Ag_{74}S_{19}(dppp)_6(fc(C\{O\}OCH_2CH_2S)_2)_{18}]$. Yield: 30 mg (63 %). Increasing the relative amount of $S(SiMe_3)_2$ in reactions led to a decreased yield of **2** and the formation of dark amorphous materials. Elemental analysis calcd. (%) for $Ag_{74}S_{55}Fe_{18}C_{450}H_{444}P_{12}O_{72}$: C 29.83, H 2.47, S 9.70; found: C 28.97, H 2.32, S 9.63.

The structure of **1** was solved with direct methods and refined using the SHELX suite of crystallographic software.[23] Crystal data for **1**: $C_{450}H_{444}Ag_{74}Fe_{18}O_{72}P_{12}S_{55}$, space group $R\bar{3}$, $a = 36.775(19)$, $b = 36.775(19)$, $c = 41.225(19)$ Å, $\gamma = 120°$, $V = 48283(42)$ Å^3, $Z = 3$, $R_1 = 0.0916$ for reflections with $I > 2\sigma(I)$, $wR_2 = 0.2639$ for all data. CCDC-1038495 (complex **1**), 1038496 $[fc(C\{O\}OCH_2CH_2Br)_2]$, 1038497 $[fc(C\{O\}OCH_2CH_2Br)COOH]$, and 1038498 $[(fc(C\{O\}O\{O\}C))_2]$ contains the supplementary crystallographic data for this paper. These data can be obtained free of charge from The Cambridge

Crystallographic Data Centre via www.ccdc.cam.ac.uk/data_request/cif. Additional supporting information is also available.

Received: December 11, 2014
Revised: February 1, 2015

Keywords: cluster compounds · iron · metallocenes · silver · structure elucidation

---

[1] a) C. Leiggener, G. Calzaferri, *Chem. Eur. J.* **2005**, *11*, 7191–7198; b) G. Calzaferri, C. Leiggener, S. Glaus, D. Schürch, K. Kuge, *Chem. Soc. Rev.* **2003**, *32*, 29–37; c) O. Fuhr, S. Dehnen, D. Fenske, *Chem. Soc. Rev.* **2013**, *42*, 1871–1906; d) H. Schmalzried, *Prog. Solid State Chem.* **1980**, *13*, 119–157.

[2] Y. Zhang, Y. Liu, C. Li, X. Chen, Q. Wang, *J. Phys. Chem. C* **2014**, *118*, 4918–4923.

[3] a) P. Jiang, C. N. Zhu, Z. L. Zhang, Z. Q. Tian, D. W. Pang, *Biomaterials* **2012**, *33*, 5130–5135; b) Y. P. Du, B. Xu, T. Fu, M. Cai, F. Li, Y. Zhang, Q. B. Wang, *J. Am. Chem. Soc.* **2010**, *132*, 1470–1471; c) C. Y. Li, Y. J. Zhang, M. Wang, Y. Zhang, G. C. Chen, L. Li, D. M. Wu, Q. B. Wang, *Biomaterials* **2014**, *35*, 393–400; d) C. X. Wang, Y. Wang, L. Xu, D. Zhang, M. X. Liu, X. W. Li, H. C. Sun, Q. Lin, B. Yang, *Small* **2012**, *8*, 3137–3142; e) Y. Zhang, G. S. Hong, Y. J. Zhang, G. C. Chen, F. Li, H. J. Dai, Q. B. Wang, *ACS Nano* **2012**, *6*, 3695–3702.

[4] a) B. K. Liu, D. J. Wang, Y. Zhang, H. M. Fan, Y. H. Lin, T. F. Jiang, T. F. Xie, *Dalton Trans.* **2013**, *42*, 2232–2237; b) Y. Zhang, B. K. Liu, D. J. Wang, Y. H. Lin, T. F. Xie, J. L. Zhai, *Mater. Chem. Phys.* **2012**, *133*, 834–838; c) S. Khanchandani, P. K. Srivastava, S. Kumar, S. Ghosh, A. K. Ganguli, *Inorg. Chem.* **2014**, *53*, 8902–8912.

[5] a) P. J. Wu, J. W. Yu, H. J. Chao, J. Y. Chang, *Chem. Mater.* **2014**, *26*, 3485–3494; b) M. H. Liu, H. C. Zeng, *Langmuir* **2014**, *30*, 9838–9849; c) R. Bose, G. Manna, S. Jana, N. Pradhan, *Chem. Commun.* **2014**, *50*, 3074–3077.

[6] C. E. Anson, A. Eichhöfer, I. Issac, D. Fenske, O. Fuhr, P. Sevillano, C. Persau, D. Stalke, J. Zhang, *Angew. Chem. Int. Ed.* **2008**, *47*, 1326–1331; *Angew. Chem.* **2008**, *120*, 1346–1351.

[7] G. Li, Z. Lei, Q. M. Wang, *J. Am. Chem. Soc.* **2010**, *132*, 17678–17679.

[8] S. Jin, S. Wang, Y. Song, M. Zhou, J. Zhong, J. Zhang, A. Xia, Y. Pei, M. Chen, P. Li, M. Zhu, *J. Am. Chem. Soc.* **2014**, *136*, 15559–15565.

[9] a) A. Desireddy, B. E. Conn, J. S. Guo, B. Yoon, R. N. Barnett, B. M. Monahan, K. Kirschbaum, W. P. Griffith, R. L. Whetten, U. Landman, T. P. Bigioni, *Nature* **2013**, *501*, 399–402; b) A. Schnepf, H. Schnöckel, *Angew. Chem. Int. Ed.* **2014**, *53*, 3064–3066; *Angew. Chem.* **2014**, *126*, 3124–3127; c) H. Y. Yang, Y. Wang, H. Q. Huang, L. Gell, L. Lehtovaara, S. Malola, H. Häkkinen, N. F. Zheng, *Nat. Commun.* **2013**, *4*, 2422–2429.

[10] a) D. G. MacDonald, J. F. Corrigan, *Philos. Trans. R. Soc. London Ser. A* **2010**, *368*, 1455–1472; b) R. Langer, B. Breitung, L. Wünsche, D. Fenske, O. Fuhr, *Z. Anorg. Allg. Chem.* **2011**, *637*, 995–1006.

[11] S. Ahmar, D. G. MacDonald, N. Vijayaratnam, T. L. Battista, M. S. Workentin, J. F. Corrigan, *Angew. Chem. Int. Ed.* **2010**, *49*, 4422–4424; *Angew. Chem.* **2010**, *122*, 4524–4526.

[12] a) A. Labande, J. Ruiz, D. Astruc, *J. Am. Chem. Soc.* **2002**, *124*, 1782–1789; b) R. C. Mulrooney, N. Singh, N. Kaur, J. F. Callan, *Chem. Commun.* **2009**, 686–688.

[13] a) K. A. Mahmoud, S. Hrapovic, J. H. T. Luong, *ACS Nano* **2008**, *2*, 1051–1057; b) M. A. Rahman, J. I. Son, M. S. Won, Y. B. Shim, *Anal. Chem.* **2009**, *81*, 6604–6611; c) R. L. Stiles, R. Balasubramanian, S. W. Feldberg, R. W. Murray, *J. Am. Chem. Soc.* **2008**, *130*, 1856–1865.

[14] a) C. Nitschke, D. Fenske, J. F. Corrigan, *Inorg. Chem.* **2006**, *45*, 9394–9401; b) A. I. Wallbank, J. F. Corrigan, *Chem. Commun.* **2001**, 377–378.

[15] M. C. Daniel, J. Ruiz, S. Nlate, J. C. Blais, D. Astruc, *J. Am. Chem. Soc.* **2003**, *125*, 2617–2628.

[16] a) Z. L. You, R. Möckel, J. Bergunde, S. Dehnen, *Chem. Eur. J.* **2014**, *20*, 13491–13496; b) G. L. Zheng, J. F. Ma, Z. M. Su, L. K. Yan, J. Yang, Y. Y. Li, J. F. Liu, *Angew. Chem. Int. Ed.* **2004**, *43*, 2409–2411; *Angew. Chem.* **2004**, *116*, 2463–2465; c) V. Chandrasekhar, S. Nagendran, S. Bansal, M. A. Kozee, D. R. Powell, *Angew. Chem. Int. Ed.* **2000**, *39*, 1833–1835; *Angew. Chem.* **2000**, *112*, 1903–1905.

[17] a) C. Pöhlker, I. Schellenberg, R. Pöttgen, S. Dehnen, *Chem. Commun.* **2010**, *46*, 2605–2607; b) Z. L. You, D. Fenske, S. Dehnen, *Dalton Trans.* **2013**, *42*, 8179–8182; c) Z. You, J. Bergunde, B. Gerke, R. Pöttgen, S. Dehnen, *Inorg Chem.* **2014**, *53*, 12512–12518.

[18] D. G. MacDonald, C. Kübel, J. F. Corrigan, *Inorg. Chem.* **2011**, *50*, 3252–3261.

[19] P. D. Beer, S. R. Bayly, *Top. Curr. Chem.* **2005**, *255*, 125–162.

[20] a) K. L. Tang, X. J. Xie, Y. H. Zhang, X. Zhao, X. L. Jin, *Chem. Commun.* **2002**, 1024–1025; b) D. Fenske, C. E. Anson, A. Eichhöfer, O. Fuhr, A. Ingendoh, C. Persau, C. Richert, *Angew. Chem. Int. Ed.* **2005**, *44*, 5242–5246; *Angew. Chem.* **2005**, *117*, 5376–5381.

[21] X. J. Wang, T. Langetepe, C. Persau, B. S. Kang, G. M. Sheldrick, D. Fenske, *Angew. Chem. Int. Ed.* **2002**, *41*, 3818–3822; *Angew. Chem.* **2002**, *114*, 3972–3977.

[22] H. Schmidbaur, A. Schier, *Angew. Chem. Int. Ed.* **2015**, *54*, 746–784; *Angew. Chem.* **2015**, *127*, 756–797.

[23] G. M. Sheldrick, *Acta Crystallogr. Sect. A* **2008**, *64*, 112–122.

Cluster Compounds

Y. Liu, B. Khalili Najafabadi,
M. Azizpoor Fard,
J. F. Corrigan* ■■■■–■■■■

A Functionalized Ag_2S Molecular Architecture: Facile Assembly ofthe Atomically Precise Ferrocene-Decorated Nanocluster$[Ag_{74}S_{19}$-$(dppp)_6(fc(C\{O\}OCH_2CH_2S)_2)_{18}]$

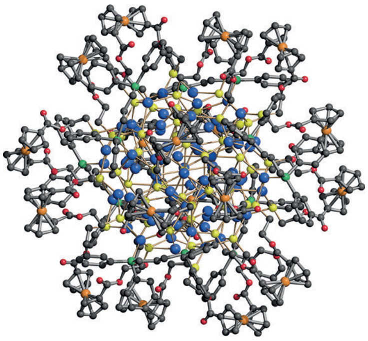

All wrapped up! A ferrocenyl-based dithiol reagent has been employed as a precursor for the preparation of a surface-functionalized $Ag_{74}S_{55}$ nanocluster $[Ag_{74}S_{19}(dppp)_6(fc(C\{O\}OCH_2CH_2S)_2)_{18}]$ (dppp = 1,3-bis(diphenylphosphino)-propane, fc = $[Fe(\eta^5\text{-}C_5H_4)_2]$). The electrochemical properties and single-crystalX-ray structure of the cluster are reported (atom colors: Ag = blue, S = yellow, P = green, O = red, Fe = orange, C = gray).